

Analysis of high-performance tensor-matrix multiplication with BLAS

Cem Savaş Başsoy^{a,*}

^a*Hamburg University of Technology, Schwarzenbergstrasse 95, 21071, Hamburg, Germany*

Abstract

The tensor-matrix multiplication is a basic tensor operation required by various tensor methods such as the ALS and the HOSVD. This paper presents flexible high-performance algorithms that compute the tensor-matrix product according to the Loops-over-GEMM (LoG) approach. Our algorithms can process dense tensors with any linear tensor layout, arbitrary tensor order and dimensions all of which can be runtime variable. We discuss different tensor slicing methods with parallelization strategies and propose six algorithm versions that call BLAS with subtensors or tensor slices. Their performance is quantified on a set of tensors with various shapes and tensor orders. Our best performing version attains a median performance of 1.37 double precision Tflops on an Intel Xeon Gold 6248R processor using Intel's MKL. We show that the tensor layout does not affect the performance significantly. Our fastest implementation is on average at least 14.05% and up to 3.79x faster than other state-of-the-art approaches and actively developed libraries like Libtorch and Eigen.

1. Introduction

Tensor computations are found in many scientific fields such as computational neuroscience, pattern recognition, signal processing and data mining [1, 2]. These computations use basic tensor operations as building blocks for decomposing and analyzing multidimensional data which are represented by tensors [3, 4]. Tensor contractions are an important subset of basic operations that need to be fast for efficiently solving tensor methods.

There are three main approaches for implementing tensor contractions. The Transpose-Transpose-GEMM-Transpose (TTGT) approach reorganizes (flattens) tensors in order to perform a tensor contraction using optimized General Matrix Multiplication (GEMM) implementations [5, 6]. Implementations of the GEMM-like Tensor-Tensor multiplication (GETT) method have macro-kernels that are similar to the ones used in fast GEMM implementations [7, 8]. The third method is the Loops-over-GEMM (LoG) approach in which BLAS are utilized with multiple tensor slices or subtensors if possible [9, 10, 11, 12]. Implementations of the LoG and TTGT approaches are in general easier to maintain and faster to port than GETT implementations which might need to adapt vector instructions or blocking parameters according to a processor's microarchitecture.

In this work, we present high-performance algorithms for the tensor-matrix multiplication which is used in many numerical methods such as the alternating least squares method [3, 4]. It is a compute-bound tensor operation and has the same arithmetic intensity as a matrix-matrix

multiplication which can almost reach the practical peak performance of a computing machine.

To our best knowledge, we are the first to combine the LoG approach described in [12, 13] for tensor-vector multiplications with the findings on tensor slicing for the tensor-matrix multiplication in [10]. Our algorithms support dense tensors with any order, dimensions and any linear tensor layout including the first- and the last-order storage formats for any contraction mode all of which can be runtime variable. They compute the tensor-matrix product in parallel using efficient GEMM or batched GEMM without transposing or flattening tensors. Despite their high performance, all algorithms are layout-oblivious and provide a sustained performance independent of the tensor layout and without tuning.

Moreover, every proposed algorithm can be implemented with less than 150 lines of c++ code where the algorithmic complexity is reduced by the BLAS implementation and the corresponding selection of subtensors or tensor slices. We have provided an open-source c++ implementation of all algorithms and a python interface for convenience. While Intel's MKL is used for our benchmarks, the user is free to select any other library that provides the BLAS interface and even integrate it's own implementation to be library independent.

The analysis in this work quantifies the impact of the tensor layout, the tensor slicing method and parallel execution of slice-matrix multiplications with varying contraction modes. The runtime measurements of our implementations are compared with state-of-the-art approaches discussed in [7, 8, 14] including Libtorch and Eigen. In summary, the main findings of our work are:

- A tensor-matrix multiplication can be implemented

*Corresponding author

Email address: cem.basoy@gmail.com (Cem Savaş Başsoy)

by an in-place algorithm with 1 GEMV and 7 GEMM calls, supporting all combinations of contraction mode, tensor order and dimensions for any linear tensor layout.

- Our fastest algorithm with tensor slices is on average 17% faster than Intel’s batched GEMM implementation when the contraction and leading dimensions of the tensors are greater than 256.
- The proposed algorithms are layout-oblivious. Their performance does not vary significantly for different tensor layouts if the contraction conditions remain the same.
- Our fastest algorithm computes the tensor-matrix multiplication on average, by at least 14.05% and up to a factor of 3.79 faster than other state-of-the-art library implementations, including LibTorch and Eigen.

The remainder of the paper is organized as follows. Section 2 presents related work. Section 3 introduces some notation on tensors and defines the tensor-matrix multiplication. Algorithm design and methods for slicing and parallel execution are discussed in Section 4. Section 5 describes the test setup. Benchmark results are presented in Section 6. Conclusions are drawn in Section 7.

2. Related Work

Springer et al. [7] present a tensor-contraction generator TCCG and the GETT approach for dense tensor contractions that is inspired from the design of a high-performance GEMM. Their unified code generator selects implementations from generated GETT, LoG and TTGT candidates. Their findings show that among 48 different contractions 15% of LoG-based implementations are the fastest.

Matthews [8] presents a runtime flexible tensor contraction library that uses GETT approach as well. He describes block-scatter-matrix algorithm which uses a special layout for the tensor contraction. The proposed algorithm yields results that feature a similar runtime behavior to those presented in [7].

Li et al. [10] introduce InTensLi, a framework that generates in-place tensor-matrix multiplication according to the LOG approach. The authors discuss optimization and tuning techniques for slicing and parallelizing the operation. With optimized tuning parameters, they report a speedup of up to 4x over the TTGT-based MATLAB tensor toolbox library discussed in [5].

Basoy [12] presents LoG-based algorithms that compute the tensor-vector product. They support dense tensors with linear tensor layouts, arbitrary dimensions and tensor order. The presented approach is to divide into eight cases calling GEMV and DOT. He reports average

speedups of 6.1x and 4.0x compared to implementations that use the TTGT and GETT approach, respectively.

Pawlowski et al. [13] propose morton-ordered blocked layout for a mode-oblivious performance of the tensor-vector multiplication. Their algorithm iterate over blocked tensors and perform tensor-vector multiplications on blocked tensors. They are able to achieve high performance and mode-oblivious computations.

3. Background

3.1. Notation

An order- p tensor is a p -dimensional array [15] where tensor elements are contiguously stored in memory. We write a , \mathbf{a} , \mathbf{A} and $\underline{\mathbf{A}}$ in order to denote scalars, vectors, matrices and tensors. If not otherwise mentioned, we assume $\underline{\mathbf{A}}$ to have order $p > 2$. The p -tuple $\mathbf{n} = (n_1, n_2, \dots, n_p)$ will be referred to as a dimension tuple with $n_r > 1$. We will use round brackets $\underline{\mathbf{A}}(i_1, i_2, \dots, i_p)$ or $\underline{\mathbf{A}}(\mathbf{i})$ to denote a tensor element where $\mathbf{i} = (i_1, i_2, \dots, i_p)$ is a multi-index. For convenience, we will also use square brackets to concatenate index tuples such that $[\mathbf{i}, \mathbf{j}] = (i_1, i_2, \dots, i_r, j_1, j_2, \dots, j_q)$ where \mathbf{i} and \mathbf{j} are multi-indices of length r and q , respectively. A subtensor is denoted by $\underline{\mathbf{A}}'$ and references elements of a tensor $\underline{\mathbf{A}}$. They are specified by a selection grid consisting of p index ranges. The index range in this work shall either address all indices of a given mode or a by a single index i_r with $1 \leq r \leq p$. Elements n'_r of a subtensor’s dimension tuple \mathbf{n}' are $n'_r = n_r$ if all indices of mode r are selected or $n'_r = 1$. We will annotate subtensors using only their non-unit modes such as $\underline{\mathbf{A}}'_{u,v,w}$ where $n_u > 1, n_v > 1$ and $n_w > 1$ and $1 \leq u \neq v \neq w \leq p$. The remaining single indices of a selection grid correspond to the loop induction variables. A subtensor is called a slice $\underline{\mathbf{A}}'_{u,v}$ if only two modes of $\underline{\mathbf{A}}$ is selected with a full range. A fiber $\underline{\mathbf{A}}'_u$ is a tensor slice with only one dimension greater than 1.

3.2. Linear Tensor Layouts

We use a layout tuple $\boldsymbol{\pi} \in \mathbb{N}^p$ to encode all linear tensor layouts including the first-order or last-order layout. They contain permuted tensor modes whose priority is given by their index. For instance, the general k -order tensor layout for an order- p tensor is given by the layout tuple $\boldsymbol{\pi}$ with $\pi_r = k - r + 1$ for $1 < r \leq k$ and r for $k < r \leq p$. The first- and last-order storage formats are given by $\boldsymbol{\pi}_F = (1, 2, \dots, p)$ and $\boldsymbol{\pi}_L = (p, p - 1, \dots, 1)$. An inverse layout tuple $\boldsymbol{\pi}^{-1}$ is defined by $\boldsymbol{\pi}^{-1}(\boldsymbol{\pi}(k)) = k$. Given a layout tuple $\boldsymbol{\pi}$ with p modes, the π_r -th element of a stride tuple is given by $w_{\pi_r} = \prod_{k=1}^{r-1} n_{\pi_k}$ for $1 < r \leq p$ and $w_{\pi_1} = 1$. Tensor elements of the π_1 -th mode are contiguously stored in memory. The location of tensor elements is determined by the tensor layout and the layout function. For a given tensor layout and stride tuple, a layout function $\lambda_{\mathbf{w}}$ maps a multi-index to a scalar index with $\lambda_{\mathbf{w}}(\mathbf{i}) = \sum_{r=1}^p w_r(i_r - 1)$, see [16, 13].

3.3. Non-Modifying Flattening and Reshaping

The flattening operation $\varphi_{r,q}$ transforms an order- p tensor $\underline{\mathbf{A}}$ to another order- p' view $\underline{\mathbf{B}}$ that has different a shape \mathbf{m} and layout τ tuple of length p' with $p' = p - q + r$ and $1 \leq r < q \leq p$. It is related to the tensor unfolding operation as defined in [4, p.459] but neither changes the element ordering nor copies tensor elements. Given a layout tuple π of $\underline{\mathbf{A}}$, the flattening operation $\varphi_{r,q}$ is defined for contiguous modes $\hat{\pi} = (\pi_r, \pi_{r+1}, \dots, \pi_q)$ of π . Let $j = 0$ if $k \leq r$ and $j = q - r$ otherwise for $1 \leq k \leq p'$. Then the resulting layout tuple $\tau = (\tau_1, \dots, \tau_{p'})$ of $\underline{\mathbf{B}}$ is given by $\tau_r = \min(\pi_{r,q})$ and $\tau_k = \pi_{k+j} - s_k$ if $k \neq r$ where $s_k = |\{\pi_i \mid \pi_{k+j} > \pi_i \wedge \pi_i \neq \min(\hat{\pi}) \wedge r \leq i \leq p\}|$. Elements of the shape tuple \mathbf{m} are defined by $m_{\tau_r} = \prod_{k=r}^q n_{\pi_k}$ and $m_{\tau_k} = n_{\pi_{k+j}}$ if $k \neq r$. Reshaping ρ transforms an order- p tensor $\underline{\mathbf{A}}$ to another order- p tensor $\underline{\mathbf{B}}$ with the shape tuple \mathbf{m} and layout tuple τ tuples, both of length p . In this work, it permutes the shape and layout tuple simultaneously without changing the element ordering and without copying tensor elements. The operation ρ is defined by a permutation tuple $\rho = (\rho_1, \dots, \rho_p)$ that defines elements of \mathbf{m} and τ with $m_r = n_{\rho_r}$ and $\tau_r = \pi_{\rho_r}$, respectively.

3.4. Tensor-Matrix Multiplication

Let $\underline{\mathbf{A}}$ and $\underline{\mathbf{C}}$ be order- p tensors with shapes $\mathbf{n}_a = ([\mathbf{n}_1, n_q, \mathbf{n}_2])$ and $\mathbf{n}_c = ([\mathbf{n}_1, m, \mathbf{n}_2])$ where $\mathbf{n}_1 = (n_1, n_2, \dots, n_{q-1})$ and $\mathbf{n}_2 = (n_{q+1}, n_{q+2}, \dots, n_p)$. Let \mathbf{B} be a matrix of shape $\mathbf{n}_b = (m, n_q)$. A q -mode tensor-matrix product is denoted by $\underline{\mathbf{C}} = \underline{\mathbf{A}} \times_q \mathbf{B}$. An element of $\underline{\mathbf{C}}$ is defined by

$$\underline{\mathbf{C}}([i_1, j, i_2]) = \sum_{i_q=1}^{n_q} \underline{\mathbf{A}}([i_1, i_q, i_2]) \cdot \mathbf{B}(j, i_q) \quad (1)$$

with $\mathbf{i}_1 = (i_1, \dots, i_{q-1})$, $\mathbf{i}_2 = (i_{q+1}, \dots, i_p)$ where $1 \leq i_r \leq n_r$ and $1 \leq j \leq m$ [10, 4]. Mode q is called the contraction mode with $1 \leq q \leq p$. The tensor-matrix multiplication generalizes the computational aspect of the two-dimensional case $\mathbf{C} = \mathbf{B} \cdot \mathbf{A}$ if $p = 2$ and $q = 1$. Its arithmetic intensity is equal to that of a matrix-matrix multiplication and is not memory-bound.

In the following, we assume that the tensors $\underline{\mathbf{A}}$ and $\underline{\mathbf{C}}$ have the same tensor layout π . Elements of matrix \mathbf{B} can be stored either in the column-major or row-major format. The tensor-matrix multiplication with i_q iterating over the second mode of \mathbf{B} is also referred to as the q -mode product which is a building block for tensor methods such as the higher-order orthogonal iteration or the higher-order singular value decomposition [4]. Please note that the following method can be applied, if indices j and i_q of matrix \mathbf{B} are swapped.

4. Algorithm Design

4.1. Baseline Algorithm with Contiguous Memory Access

The tensor-times-matrix multiplication in equation 1 can be implemented with one sequential algorithm using a

```

1 ttm( $\underline{\mathbf{A}}, \underline{\mathbf{B}}, \underline{\mathbf{C}}, \mathbf{n}, \mathbf{i}, m, q, \hat{q}, r$ )
2   if  $r = \hat{q}$  then
3     | ttm( $\underline{\mathbf{A}}, \underline{\mathbf{B}}, \underline{\mathbf{C}}, \mathbf{n}, \mathbf{i}, m, q, \hat{q}, r - 1$ )
4   else if  $r > 1$  then
5     | for  $i_{\pi_r} \leftarrow 1$  to  $n_{\pi_r}$  do
6       | | ttm( $\underline{\mathbf{A}}, \underline{\mathbf{B}}, \underline{\mathbf{C}}, \mathbf{n}, \mathbf{i}, m, q, \hat{q}, r - 1$ )
7   else
8     | for  $j \leftarrow 1$  to  $m$  do
9       | | for  $i_q \leftarrow 1$  to  $n_q$  do
10        | | | for  $i_{\pi_1} \leftarrow 1$  to  $n_{\pi_1}$  do
11          | | | |  $\underline{\mathbf{C}}([i_1, j, i_2]) += \underline{\mathbf{A}}([i_1, i_q, i_2]) \cdot \mathbf{B}(j, i_q)$ 

```

Algorithm 1: Modified baseline algorithm with contiguous memory access for the tensor-matrix multiplication. The tensor order p must be greater than 1 and the contraction mode q must satisfy $1 \leq q \leq p$ and $\pi_1 \neq q$. The initial call must happen with $r = p$ where \mathbf{n} is the shape tuple of $\underline{\mathbf{A}}$ and m is the q -th dimension of $\underline{\mathbf{C}}$.

nested recursion [16]. It consists of two **if** statements with an **else** branch that computes a fiber-matrix product with two loops. The outer loop iterates over the dimension m of $\underline{\mathbf{C}}$ and \mathbf{B} , while the inner iterates over dimension n_q of $\underline{\mathbf{A}}$ and \mathbf{B} computing an inner product with fibers of $\underline{\mathbf{A}}$ and \mathbf{B} . While matrix \mathbf{B} can be accessed contiguously depending on its storage format, elements of $\underline{\mathbf{A}}$ and $\underline{\mathbf{C}}$ are accessed non-contiguously if $\pi_1 \neq q$.

A better approach is illustrated in algorithm 1 where the loop order is adjusted to the tensor layout π and memory is accessed contiguously for $\pi_1 \neq q$ and $p > 1$. The adjustment of the loop order is accomplished in line 5 which uses the layout tuple π to select a multi-index element i_{π_r} and to increment it with the corresponding stride w_{π_r} . Hence, with increasing recursion level and decreasing r , indices are incremented with smaller strides as $w_{\pi_r} \leq w_{\pi_{r+1}}$. The second **if** statement in line number 4 allows the loop over mode π_1 to be placed into the base case which contains three loops performing a slice-matrix multiplication. In this way, the inner-most loop is able to increment i_{π_1} with a unit stride and contiguously accesses tensor elements of $\underline{\mathbf{A}}$ and $\underline{\mathbf{C}}$. The second loop increments i_q with which elements of \mathbf{B} are contiguously accessed if \mathbf{B} is stored in the row-major format. The third loop increments j and could be placed as the second loop if \mathbf{B} is stored in the column-major format.

While spatial data locality is improved by adjusting the loop ordering, slices $\underline{\mathbf{A}}'_{\pi_1, q}$, fibers $\underline{\mathbf{C}}'_{\pi_1}$ and elements $\underline{\mathbf{B}}(j, i_q)$ are accessed m , n_q and n_{π_1} times, respectively. The specified fiber of $\underline{\mathbf{C}}$ might fit into first or second level cache, slice elements of $\underline{\mathbf{A}}$ are unlikely to fit in the local caches if the slice size $n_{\pi_1} \times n_q$ is large, leading to higher cache misses and suboptimal performance. Instead of optimizing for better temporal data locality, we use existing high-performance BLAS implementations for the base case. The following subsection explains this approach.

Case	Order p	Layout $\pi_{\underline{\mathbf{A}}, \underline{\mathbf{C}}}$	Layout $\pi_{\mathbf{B}}$	Mode q	Routine	T	M	N	K	A	LDA	B	LDB	LDC
1	1	-	rm/cm	1	gemv	-	m	n_1	-	$\underline{\mathbf{B}}$	n_1	$\underline{\mathbf{A}}$	-	-
2	2	cm	rm	1	gemm	\mathbf{B}	n_2	m	n_1	$\underline{\mathbf{A}}$	n_1	\mathbf{B}	n_1	m
	2	cm	cm	1	gemm	-	m	n_2	n_1	$\underline{\mathbf{B}}$	m	$\underline{\mathbf{A}}$	n_1	m
3	2	cm	rm	2	gemm	-	m	n_1	n_2	\mathbf{B}	n_2	$\underline{\mathbf{A}}$	n_1	n_1
	2	cm	cm	2	gemm	\mathbf{B}	n_1	m	n_2	$\underline{\mathbf{A}}$	n_1	\mathbf{B}	m	n_1
4	2	rm	rm	1	gemm	-	m	n_2	n_1	\mathbf{B}	n_1	$\underline{\mathbf{A}}$	n_2	n_2
	2	rm	cm	1	gemm	\mathbf{B}	n_2	m	n_1	$\underline{\mathbf{A}}$	n_2	\mathbf{B}	m	n_2
5	2	rm	rm	2	gemm	\mathbf{B}	n_1	m	n_2	$\underline{\mathbf{A}}$	n_2	\mathbf{B}	n_2	m
	2	rm	cm	2	gemm	-	m	n_1	n_2	\mathbf{B}	m	$\underline{\mathbf{A}}$	n_2	m
6	> 2	any	rm	π_1	gemm	\mathbf{B}	\bar{n}_q	m	n_q	$\underline{\mathbf{A}}$	n_q	\mathbf{B}	n_q	m
	> 2	any	cm	π_1	gemm	-	m	\bar{n}_q	n_q	\mathbf{B}	m	$\underline{\mathbf{A}}$	n_q	m
7	> 2	any	rm	π_p	gemm	-	m	\bar{n}_q	n_q	\mathbf{B}	n_q	$\underline{\mathbf{A}}$	\bar{n}_q	\bar{n}_q
	> 2	any	cm	π_p	gemm	\mathbf{B}	\bar{n}_q	m	n_q	$\underline{\mathbf{A}}$	\bar{n}_q	\mathbf{B}	m	\bar{n}_q
8	> 2	any	rm	π_2, \dots, π_{p-1}	gemm*	-	m	n_{π_1}	n_q	\mathbf{B}	n_q	$\underline{\mathbf{A}}$	w_q	w_q
	> 2	any	cm	π_2, \dots, π_{p-1}	gemm*	\mathbf{B}	n_{π_1}	m	n_q	$\underline{\mathbf{A}}$	w_q	\mathbf{B}	m	w_q

Table 1: Eight cases with `gemv` and `gemm` for the mode- q tensor-matrix multiplication. Arguments T, M, N, etc. of the BLAS are chosen with respect to the tensor order p , layout π of $\underline{\mathbf{A}}$, \mathbf{B} , $\underline{\mathbf{C}}$ and contraction mode q where T specifies if \mathbf{B} is transposed. `gemm*` denotes multiple `gemm` calls with different tensor slices. Argument \bar{n}_q for case 6 and 7 is given by $\bar{n}_q = (\prod_r n_r)/n_q$. The input matrix \mathbf{B} is either stored in column-major cm or row-major rm order.

4.2. BLAS-based Algorithms with Tensor Slices

Algorithm 1 computes the mode- q tensor-matrix product in a recursive fashion. The base case multiplies different tensor slices of $\underline{\mathbf{A}}$ with the matrix \mathbf{B} . Instead of optimizing the slice-matrix multiplication in the base case, one can use a `gemm` routine instead. Note that algorithm 1 is the general case for $p \geq 2$ but only executable for $\pi_1 \neq q$. For $\pi_1 = q$, the tensor-matrix product can be computed by a matrix-matrix multiplication where the input tensor $\underline{\mathbf{A}}$ can be flattened into a matrix without any copy operation. The same can be applied when $\pi_p = q$ and five other cases where the input tensor is either one or two-dimensional. In summary, there are seven other corner cases to the general case where a single `gemv` or `gemm` call suffices to compute the tensor-matrix product. All eight cases are listed in table 1. The arguments of `gemv` or `gemm` are set according to the tensor order p , tensor layout π and contraction mode q . If the input matrix \mathbf{B} has the row-major order, parameter `Cblas_ORDER` of function `gemm` is set to `CblasRowMajor` and `CblasColMajor` otherwise. Note that table 1 supports all linear tensor layouts of $\underline{\mathbf{A}}$ and $\underline{\mathbf{C}}$ with no limitations on tensor order and contraction mode. The following subsection describes all eight cases when the input matrix \mathbf{B} has the row-major order.

4.2.1. Row-Major Matrix Multiplication

Case 1: If $p = 1$, The tensor-vector product $\underline{\mathbf{A}} \times_1 \mathbf{B}$ can be computed with a `gemv` operation where $\underline{\mathbf{A}}$ is an order-1 tensor \mathbf{a} of length n_1 such that $\mathbf{a}^T \cdot \mathbf{B}$.

Case 2-5: If $p = 2$, $\underline{\mathbf{A}}$ and $\underline{\mathbf{C}}$ are order-2 tensors with dimensions n_1 and n_2 . In this case the tensor-matrix product can be computed with a single `gemm`. If $\underline{\mathbf{A}}$ and $\underline{\mathbf{C}}$ have the column-major format with $\pi = (1, 2)$, `gemm` either executes $\mathbf{C} = \underline{\mathbf{A}} \cdot \mathbf{B}^T$ for $q = 1$ or $\mathbf{C} = \mathbf{B} \cdot \underline{\mathbf{A}}$ for $q = 2$. Reshaping both matrices using ρ with $\rho = (2, 1)$, `gemm` interprets $\underline{\mathbf{C}}$ and $\underline{\mathbf{A}}$ as matrices in row-major format although both

are stored column-wise. If $\underline{\mathbf{A}}$ and $\underline{\mathbf{C}}$ have the row-major format with $\pi = (2, 1)$, `gemm` either executes $\mathbf{C} = \mathbf{B} \cdot \underline{\mathbf{A}}$ for $q = 1$ or $\mathbf{C} = \underline{\mathbf{A}} \cdot \mathbf{B}^T$ for $q = 2$. The transposition of \mathbf{B} is necessary for the cases 2 and 5 which is independent of the chosen layout.

Case 6-7 : If $p > 2$ and if $q = \pi_1$ (case 6), a single `gemm` with the corresponding arguments executes $\mathbf{C} = \underline{\mathbf{A}} \cdot \mathbf{B}^T$ and computes a tensor-matrix product $\underline{\mathbf{C}} = \underline{\mathbf{A}} \times_{\pi_1} \mathbf{B}$. Tensors $\underline{\mathbf{A}}$ and $\underline{\mathbf{C}}$ are flattened with $\varphi_{2,p}$ to row-major matrices \mathbf{A} and \mathbf{C} . Matrix \mathbf{A} has $\bar{n}_{\pi_1} = \bar{n}/n_{\pi_1}$ rows and n_{π_1} columns while matrix \mathbf{C} has the same number of rows and m columns. If $\pi_p = q$ (case 7), $\underline{\mathbf{A}}$ and $\underline{\mathbf{C}}$ are flattened with $\varphi_{1,p-1}$ to column-major matrices \mathbf{A} and \mathbf{C} . Matrix \mathbf{A} has n_{π_p} rows and $\bar{n}_{\pi_p} = \bar{n}/n_{\pi_p}$ columns while \mathbf{C} has m rows and the same number of columns. In this case, a single `gemm` executes $\mathbf{C} = \mathbf{B} \cdot \underline{\mathbf{A}}$ and computes $\underline{\mathbf{C}} = \underline{\mathbf{A}} \times_{\pi_p} \mathbf{B}$. Noticeably, the desired contraction are performed without copy operations, see subsection 3.3.

Case 8 ($p > 2$): If the tensor order is greater than 2 with $\pi_1 \neq q$ and $\pi_p \neq q$, the modified baseline algorithm 1 is used to successively call $\bar{n}/(n_q \cdot n_{\pi_1})$ times `gemm` with different tensor slices of $\underline{\mathbf{C}}$ and $\underline{\mathbf{A}}$. Each `gemm` computes one slice $\underline{\mathbf{C}}'_{\pi_1, q}$ of the tensor-matrix product $\underline{\mathbf{C}}$ using the corresponding tensor slices $\underline{\mathbf{A}}'_{\pi_1, q}$ and the matrix \mathbf{B} . The matrix-matrix product $\mathbf{C} = \mathbf{B} \cdot \underline{\mathbf{A}}$ is performed by interpreting both tensor slices as row-major matrices \mathbf{A} and \mathbf{C} which have the dimensions (n_q, n_{π_1}) and (m, n_{π_1}) , respectively.

4.2.2. Column-Major Matrix Multiplication

The tensor-matrix multiplication is performed with the column-major version of `gemm` when the input matrix \mathbf{B} is stored in column-major order. Although the number of `gemm` cases remains the same, the `gemm` arguments must be rearranged. The argument arrangement for the column-major version can be derived from the row-major version

by swapping the BLAS arguments of \mathbf{M} and \mathbf{N} , as well as \mathbf{A} and \mathbf{B} . Additionally, the transposition flag for matrix \mathbf{B} is toggled and the leading dimension argument of \mathbf{A} is swapped to LDB or LDA as well. The only new argument is the new leading dimension of \mathbf{B} . Given case 4 with the row-major matrix multiplication in table 1 where tensor $\underline{\mathbf{A}}$ and matrix \mathbf{B} are passed to \mathbf{B} and \mathbf{A} . The corresponding column-major version is attained when tensor $\underline{\mathbf{A}}$ and matrix \mathbf{B} are passed to \mathbf{A} and \mathbf{B} where the transpose flag for \mathbf{B} is set and the remaining dimensions are adjusted accordingly.

4.2.3. Matrix Multiplication Variations

The column-major and row-major versions of `gemm` can be used interchangeably by adapting the storage format. This means that a `gemm` operation for column-major matrices can compute the same matrix product as one for row-major matrices, provided the arguments are rearranged accordingly. While the argument rearrangement is similar to the previously outlined one, the arguments associated with the matrices \mathbf{A} and \mathbf{B} are interchanged. Specifically, LDA and LDB as well as \mathbf{M} and \mathbf{N} are swapped, along with the corresponding matrix pointers. In addition, the transposition flag must be set for \mathbf{A} or \mathbf{B} in the new format if \mathbf{B} or \mathbf{A} is transposed in the original version.

Given case 4 with the column-major matrix multiplication in table 1 where tensor $\underline{\mathbf{A}}$ and matrix \mathbf{B} are set for \mathbf{A} and \mathbf{B} and \mathbf{B} is transposed. Then the arguments of an equivalent row-major multiplication for \mathbf{A} , \mathbf{B} , \mathbf{M} , \mathbf{N} , LDA, LDB and τ are \mathbf{B} , $\underline{\mathbf{A}}$, m , n_2 , m , n_2 and \mathbf{B} . Another possible matrix multiplication variant that yields the same product is computed when, instead of \mathbf{B} , both tensors $\underline{\mathbf{A}}$ and $\underline{\mathbf{C}}$ are transposed and their corresponding arguments are adjusted accordingly. However, we assume that such reformulations of the matrix multiplication do not outperform the variants shown in Table 1, as we expect the use of highly optimized BLAS libraries.

4.3. BLAS-Based Algorithms with Subtensors

The eighth case can be further optimized by slicing larger subtensors and use additional dimensions for the slice-matrix multiplication. The selected dimensions must adhere to flatten the subtensor into a matrix without re-ordering or copying elements, see lemma 4.1 in [10]. The number of additional modes is $\hat{q} - 1$ with $\hat{q} = \pi^{-1}(q)$ and the corresponding modes are $\pi_1, \pi_2, \dots, \pi_{\hat{q}-1}$. Applying flattening $\varphi_{1, \hat{q}-1}$ and reshaping ρ with $\rho = (2, 1)$ on a subtensor of $\underline{\mathbf{A}}$ yields a row-major matrix \mathbf{A} with shape $(n_q, \prod_{r=1}^{\hat{q}-1} n_{\pi_r})$. Analogously, tensor $\underline{\mathbf{C}}$ becomes a row-major matrix with the shape $(m, \prod_{r=1}^{\hat{q}-1} n_{\pi_r})$. This description supports all linear tensor layouts and generalizes lemma 4.2 in [10].

Algorithm 1 needs a minor modification so that `gemm` can be used with flattened subtensors instead of tensor slices. The non-base case of the modified algorithm only iterates over dimensions with indices that are larger than \hat{q} , omitting the first \hat{q} modes $\pi_{1, \hat{q}} = (\pi_1, \dots, \pi_{\hat{q}})$ with $\pi_{\hat{q}} = q$.

The conditions in line 2 and 4 are changed to $1 < r \leq \hat{q}$ and $\hat{q} < r$, respectively. The single indices of the subtensors $\underline{\mathbf{A}}'_{\pi_{1, \hat{q}}}$ and $\underline{\mathbf{C}}'_{\pi_{1, \hat{q}}}$ are given by the loop induction variables that belong to the π_r -th loop with $\hat{q} + 1 \leq r \leq p$.

4.4. Parallel BLAS-based Algorithms

Next, three parallel approaches for the eighth case. Note that cases 1 to 7 already call a multi-threaded `gemm`.

4.4.1. Sequential Loops and Parallel Matrix Multiplication

A simple approach is to not modify algorithm 1 and sequentially call a multi-threaded `gemm` in the base case as described in subsection 4.2. This is beneficial if $q = \pi_{p-1}$, the inner dimensions n_{π_1}, \dots, n_q are large or if the outer-most dimension n_{π_p} is smaller than the available processor cores. However, when the above conditions are not met, the algorithm executes multi-threaded `gemm` with small subtensors. This might lead to a low utilization of available computational resources. This algorithm version will be referred to as `<seq-loops, par-gemm>`.

4.4.2. Parallel Loops and Multithreaded Matrix Multiplication

A more advanced version of the above algorithm executes a single-threaded `gemm` in parallel with all available (free) modes. The number of free modes depends on the tensor slicing. If subtensors are used, all $\pi_{\hat{q}+1}, \dots, \pi_p$ modes are free and can be used for parallel execution. In case of tensor slices, only dimensions with indices π_1 and $\pi_{\hat{q}}$ are free.

Using tensor slices for the multiplication, $\underline{\mathbf{A}}$ and $\underline{\mathbf{C}}$ are flattened twice with $\varphi_{\pi_{\hat{q}+1}, \pi_p}$ and $\varphi_{\pi_2, \pi_{\hat{q}-1}}$. The flattened tensors are of order 4 with dimensions $n_{\pi_1}, \hat{n}_{\pi_2}, n_q$ or m, \hat{n}_{π_4} where $\hat{n}_{\pi_2} = \prod_{r=2}^{\hat{q}-1} n_{\pi_r}$ and $\hat{n}_{\pi_4} = \prod_{r=\hat{q}+1}^p n_{\pi_r}$. This approach transforms the tree-recursion into two loops. The outer loop iterates over \hat{n}_{π_4} while the inner loop iterates over \hat{n}_{π_2} calling `gemm` with slices $\underline{\mathbf{A}}'_{\pi_{1, \hat{q}}}$ and $\underline{\mathbf{C}}'_{\pi_{1, \hat{q}}}$. Both loops are parallelized using `omp parallel for` together with the `collapse(2)` and the `num_threads` clause which specifies the thread number.

If subtensors are used, both tensors are flattened twice with $\varphi_{\pi_{\hat{q}+1}, \pi_p}$ and $\varphi_{\pi_1, \pi_{\hat{q}-1}}$. The flattened tensors are of order 3 with dimensions \hat{n}_{π_1}, n_q or m, \hat{n}_{π_4} where $\hat{n}_{\pi_1} = \prod_{r=1}^{\hat{q}-1} n_{\pi_r}$ and $\hat{n}_{\pi_4} = \prod_{r=\hat{q}+1}^p n_{\pi_r}$. The corresponding algorithm consists of one loops which iterates over \hat{n}_{π_4} calling single-threaded `gemm` with multiple subtensors $\underline{\mathbf{A}}'_{\pi', q}$ and $\underline{\mathbf{C}}'_{\pi', q}$ with $\pi' = (\pi_1, \dots, \pi_{\hat{q}-1})$.

Both algorithm variants will be referred to as `<par-loops, seq-gemm>` which can be used with subtensors or tensor slices. Note that `<seq-loops, par-gemm>` and `<par-loops, seq-gemm>` are opposing versions where either `gemm` or the free loops are performed in parallel. The all-parallel version `<par-loops, par-gemm>` executes available loops in parallel where each loop thread executes a multi-threaded `gemm` with either subtensors or tensor slices.

4.4.3. Multithreaded Batched Matrix Multiplication

The next version of the base algorithm is a modified version of the general subtensor-matrix approach that calls a single batched `gemm` for the eighth case. The subtensor dimensions and remaining `gemm` arguments remain the same. The library implementation is responsible how subtensor-matrix multiplications are executed and if subtensors are further divided into smaller subtensors or tensor slices. This version will be referred to as the `<gemm_batch>` variant.

5. Experimental Setup

5.0.1. Computing System

The experiments have been carried out on an Intel Xeon Gold 6248R processor with a Cascade micro-architecture. The processor consists of 24 cores operating at a base frequency of 3 GHz. With 24 cores and a peak AVX-512 boost frequency of 2.5 GHz, the processor achieves a theoretical data throughput of ca. 1.92 double precision Tflops. We measured a peak performance of 1.78 double precision Tflops using the likwid performance tool.

We have used the GNU compiler v10.2 with the highest optimization level `-O3` and `-march=native`, `-pthread` and `-fopenmp`. Loops within for the eighth case have been parallelized using GCC’s OpenMP v4.5 implementation. We have used the `gemv` and `gemm` implementation of the 2024.0 Intel MKL and its own threading library `mkl_intel_thread` together with the threading runtime library `libiomp5`.

If not otherwise mentioned, both tensors **A** and **C** are stored according to the first-order tensor layout. Matrix **B** has the row-major storage format.

5.0.2. Tensor Shapes

We have used asymmetrically and symmetrically shaped tensors in order to cover many use cases. The dimension tuples of both shape types are organized within two three-dimensional arrays with which tensors are initialized. The dimension array for the first shape type contains $720 = 9 \times 8 \times 10$ dimension tuples where the row number is the tensor order ranging from 2 to 10. For each tensor order, 8 tensor instances with increasing tensor size is generated. A special feature of this test set is that the contraction dimension and the leading dimension are disproportionately large. The second set consists of $336 = 6 \times 8 \times 7$ dimensions tuples where the tensor order ranges from 2 to 7 and has 8 dimension tuples for each order. Each tensor dimension within the second set is 2^{12} , 2^8 , 2^6 , 2^5 , 2^4 and 2^3 . A detailed explanation of the tensor shape setup is given in [12, 16].

6. Results and Discussion

6.1. Slicing Methods

The next paragraphs analyze the two proposed slicing methods and discuss runtime results of `<par-loops,seq-gemm>`

and `<gemm_batch>` using asymmetrically and symmetrically shaped tensors. Fig. 1 contains six contour plots (performance maps) in which `<par-loops,seq-gemm>` either uses subtensors or tensor slices and `<gemm_batch>` loops over subtensors only. Every performance value within the maps represent a mean value that has been averaged over tensor sizes for a tensor order¹.

For asymmetrically shaped tensors, function `<par-loops,seq-gemm>` with tensor slices performs on average 18% better than with subtensors and is on average 11% faster than Intel’s `gemm_batch` routine. It reaches almost 1.1 Tflops for non-edge cases with $q > 2$ and $p > 6$. This suggests that the Intel’s implementation does not divide subtensors into smaller blocks.

With symmetrically shaped tensors, `<par-loops,seq-gemm>` with tensor slices and `<gemm_batch>` almost show the same runtime behavior, reaching 221.52 Gflops and 236.21 Gflops, respectively. Moreover, the slicing method seems to have only little affect on the performance of `<par-loops,seq-gemm>`. In contrast to the performance maps with asymmetrically shaped tensors, all functions almost reach the attainable peak performance of 1.7 Tflops when $p = 2$. This can be by the fact that both dimensions are equal or larger than 4096 enabling `gemm` to operate under optimal conditions.

6.2. Parallelization Methods

The contour plots in Fig. 1 contain performance data of all cases except for 4 and 5, see Table ?? . The effects of the presented slicing and parallelization methods can be better understood if performance data of only the eighth case is examined. Fig. 2 contains cumulative performance distributions of all the proposed algorithms which are generated `gemm` or `gemm_batch` calls within case 8. As the distribution is empirically computed, the probability y of a point (x, y) on a distribution function corresponds to the number of test cases of a particular algorithm that achieves x or less Tflops. For instance, function `<seq-loops,par-gemm>` with subtensors computes the tensor-matrix product for 50% percent of the test cases with equal to or less than 0.6 Tflops in case of asymmetrically shaped tensor. Consequently, distribution functions with an exponential growth are favorable while logarithmic behavior is less desirable. The test set cardinality for case 8 is 255 for asymmetrically shaped tensors and 91 for symmetrically ones.

In case of asymmetrically shaped tensors, `<par-loops,seq-gemm>` with tensor slices performs best and outperforms `<gemm_batch>`. One unexpected finding is that function `<seq-loops,par-gemm>` with any slicing strategy performs better than `<gemm_batch>` when the tensor order p and contraction mode q satisfy $4 \leq p \leq 7$ and $2 \leq q \leq 4$, respectively. Functions executed with symmetrically shaped tensors reach at most 743 Gflops for the eighth case which is less than half of the attainable peak performance of 1.7 Tflops. This is

¹Note that Fig. 2 suggests that the contraction mode q can be greater than p which is not possible. Our profiling program sets $q = p$ in such cases.

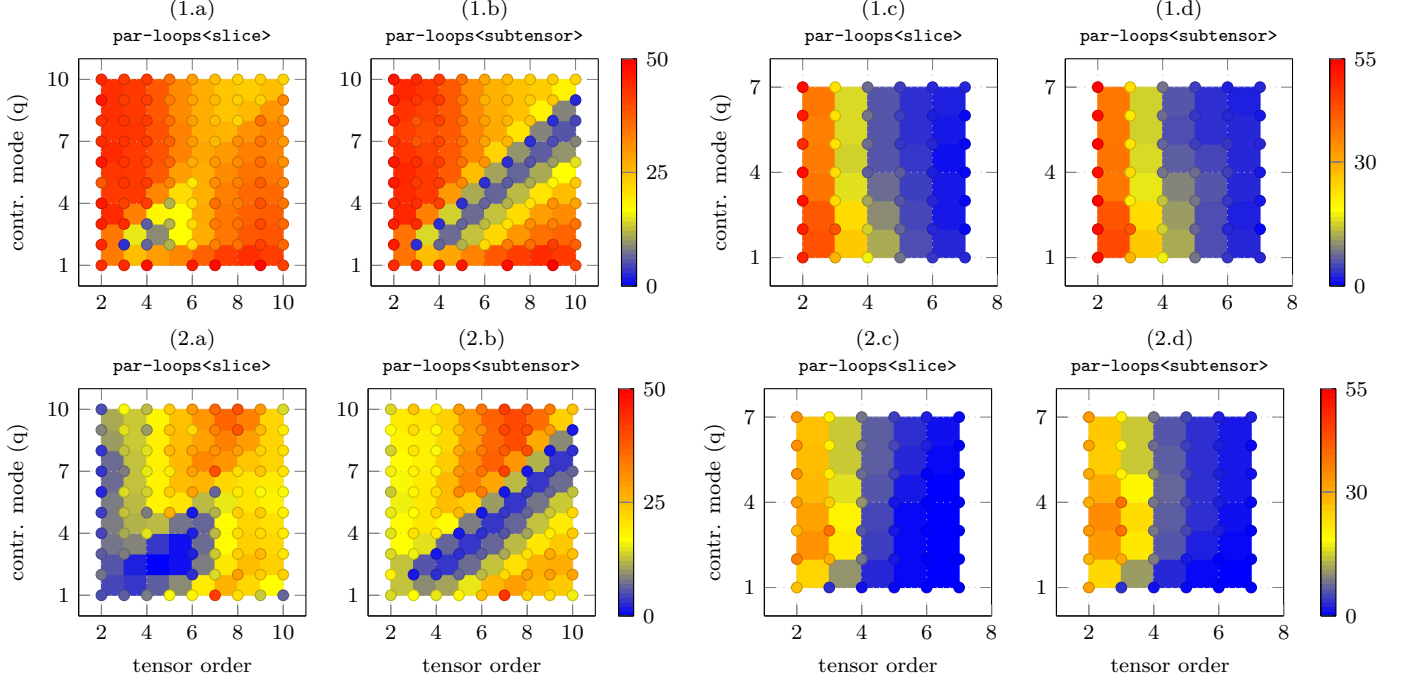


Figure 1: Performance maps of the TTM in double-precision Gflops per core of the proposed algorithms with varying tensor orders p and contraction modes q . The top row of maps (1.) are measured on an Intel Xeon Gold 5318Y with MKL routines while bottom row of maps with number (2.) are measured on an AMD EPYC 9354 with AOCL routines. Tensors are asymmetrically shaped on the left four maps (a,b) and symmetrically shaped on the right four maps (c,d). Tensor \mathbf{C} and \mathbf{C} have the first-order while \mathbf{B} has the second-order storage format (row-major).

expected as cases 2 and 3 are not considered. Functions `<par-loops,seq-gemm>` with subtensors and `<gemm_batch>` have almost the same performance distribution outperforming `<seq-loops,par-gemm>` for almost every test case. Function `<par-loops,seq-gemm>` with tensor slices is on average almost as fast as with subtensors. However, if the tensor order is greater than 3 and the tensor dimensions are less than 64, its running time increases by almost a factor of 2.

These observations suggest to use `<par-loops,seq-gemm>` with tensor slices for common cases in which the leading and contraction dimensions are larger than 64 elements. Subtensors should only be used if the leading dimension n_{π_1} of $\mathbf{A}_{\pi_1,q}$ and $\mathbf{C}_{\pi_1,q}$ falls below 64. This strategy is different to the one presented in [10] that maximizes the number of modes involved in the matrix multiply. We have also observed no performance improvement if `par-gemm` was used with `par-loops` which is why their distribution functions are not shown in Fig. 2. Moreover, in most cases the `seq-loops` implementations are independent of the tensor shape slower than `par-loops`, even for smaller tensor slices.

6.3. Layout-Oblivious Algorithms

Fig. 3 contains two subfigures visualizing performance statics in double-precision Tflops of `<gemm_batch>` (left subfigure) and `<par-loops,seq-gemm>` with subtensors (right subfigure). Each box plot with the number k has been computed from benchmark data with symmetrically shaped order-7 tensors with the k -order tensor layout. The 1-

order and 7-order layout, for instance, are the first- and last-order storage formats for the order-7 tensor with $\pi_F = (1, 2, \dots, 7)$ and $\pi_L = (7, 6, \dots, 1)$. The definition of k -order tensor layouts can be found in section 3.2.

The low performance of around 70 Gflops can be attributed to the fact that the contraction dimension of subtensors of tensor slices of symmetrically shaped order-7 tensors are 8 while the leading dimension is 8 or at most 48 for subtensors. The relative standard deviation of `<gemm_batch>`'s and `<par-loops,seq-gemm>`'s median values are 12.95% and 17.61%. Their respective interquartile range are similar with a relative standard deviation of 22.25% and 15.23%.

The runtime results with different k -order tensor layouts show that the performance of our proposed algorithms is not designed for a specific tensor layout. Moreover, the performance stays within an acceptable range independent of the tensor layout.

6.4. Comparison with other Approaches

We have compared the best performing algorithm with four libraries that implement the tensor-matrix multiplication.

Library `tcl` implements the TTGT approach with a high-perform tensor-transpose library `hptt` which is discussed in [7]. `tblis` implements the GETT approach that is akin to Blis' algorithm design for the matrix multiplication [8]. The tensor extension of `eigen` (v3.3.7) is used by the Tensorflow framework. Library `libtorch` (v2.3.0)

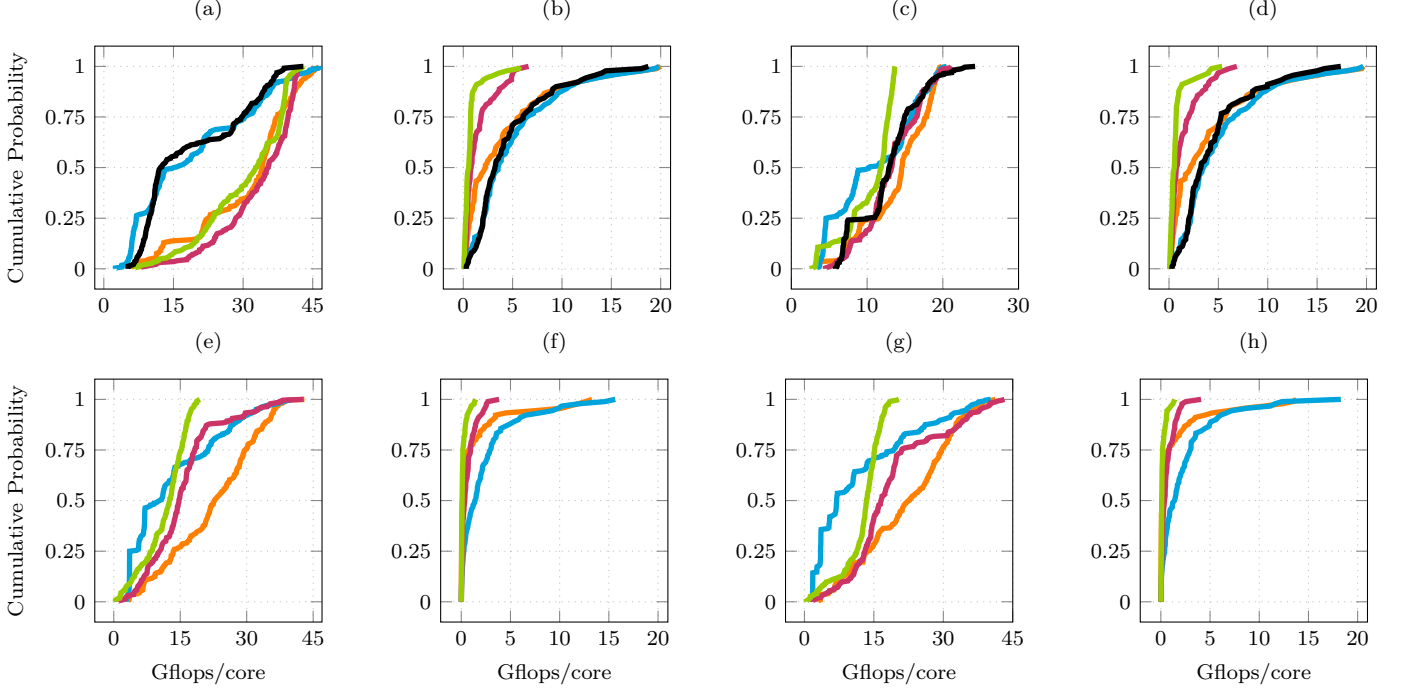


Figure 2: Cumulative performance distributions of the proposed algorithms for the eighth case. Each distribution line belongs to one algorithm: $\langle \text{gemm_batch} \rangle$ (—), $\langle \text{seq-loops,par-gemm} \rangle$ (—) and $\langle \text{par-loops,seq-gemm} \rangle$ (—) using tensor slices, $\langle \text{seq-loops,par-gemm} \rangle$ (—) and $\langle \text{par-loops,seq-gemm} \rangle$ (—) using subtenors. Tensors are asymmetrically (left plot) and symmetrically shaped (right plot).

is the c++ distribution of PyTorch. **tlb** denotes our library using algorithm $\langle \text{par-loops,seq-gemm} \rangle$ that have been presented in the previous paragraphs.

Fig. 2 contains cumulative performance distributions for the complete test sets comparing the performance distribution of our implementation with the previously mentioned libraries. Note that we only have used tensor slices for asymmetrically shaped tensors (left plot) and subtenors for symmetrically shaped tensors (right plot). Our implementation with a median performance of 793.75 Gflops outperforms others’ for almost every asymmetrically shaped tensor in the test set. The median performances of tcl, tlbis, libtorch and eigen are 503.61, 415.33, 496.22 and 244.69 Gflops reaching on average 74.11%, 61.14%, 76.68% and 39.34% of tlib’s throughputs.

In case of symmetrically shaped tensors the performance distributions of all libraries on the right plot in Fig. 2 are much closer. The median performances of tlib, tlbis, libtorch and eigen are 228.93, 208.69, 76.46, 46.25 Gflops reaching on average 73.06%, 38.89%, 19.79% of tlib’s throughputs². All libraries operate with 801.68 or less Gflops for the cases 2 and 3 which is almost half of tlib’s performance with 1579 Gflops. The median performance and the interquartile range of tlbis and tlib for the cases 6 and 7 are almost the same. Their respective median Gflops are 255.23 and 263.94 for the sixth case and 121.17

and 144.27 for the seventh case. This explains the similar performance distributions when their performance is less than 400 Gflops. Libtorch and eigen compute the tensor-matrix product, in median, with 17.11 and 9.64 Gflops/s, respectively. Our library tlib has a median performance of 102.11 Gflops and outperforms tlbis with 79.35 Gflops for the eighth case.

7. Conclusion and Future Work

We presented efficient layout-oblivious algorithms for the compute-bound tensor-matrix multiplication which is essential for many tensor methods. Our approach is based on the LOG-method and computes the tensor-matrix product in-place without transposing tensors. It applies the flexible approach described in [12] and generalizes the findings on tensor slicing in [10] for linear tensor layouts. The resulting algorithms are able to process dense tensors with arbitrary tensor order, dimensions and with any linear tensor layout all of which can be runtime variable.

Our benchmarks show that dividing the base algorithm into eight different GEMM cases improves the overall performance. We have demonstrated that algorithms with parallel loops over single-threaded GEMM calls with tensor slices and subtenors perform best. Interestingly, they outperform a single batched GEMM with subtenors, on average, by 14% in case of asymmetrically shaped tensors and if tensor slices are used. Both version computes the tensor-matrix product on average faster than other state-

²We were unable to run tcl with our test set containing symmetrically shaped tensors. We suspect a very high memory demand to be the reason.

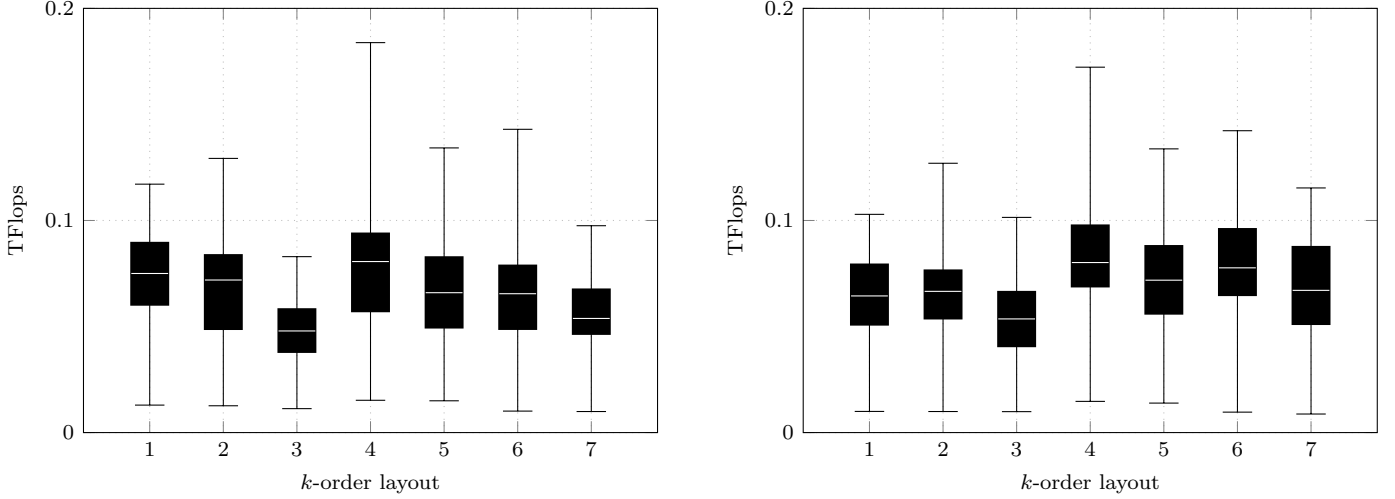


Figure 3: Box plots visualizing performance statics in double-precision Tflops of `<gemm_batch>` (left) and `<par-loops,seq-gemm>` with sub-tensors (right). Box plot number k denotes the k -order tensor layout of symmetrically shaped tensors with order 7.

of-the-art implementations. We have shown that our algorithms are layout-oblivious and do not need further refinement if the tensor layout is changed. We measured a relative standard deviation of 12.95% and 17.61% with symmetrically-shaped tensors for different k -order tensor layouts.

One can conclude that LOG-based tensor-times-matrix algorithms are on par or can even outperform TTGT-based and GETT-based implementations without loosing their flexibility. Hence, other actively developed libraries such as LibTorch and Eigen might benefit from implementing the proposed algorithms. Our header-only library provides `c++` interfaces and a python module which allows frameworks to easily integrate our library.

In the near future, we intend to incorporate our implementations in TensorLy, a widely-used framework for tensor computations [17, 18]. Currently, we lack a heuristic for selecting subtensor sizes and choosing the corresponding algorithm. Using the insights provided in [10] could help to further increase the performance. Additionally, we want to explore to what extend our approach can be applied for the general tensor contractions.

7.0.1. Source Code Availability

Project description and source code can be found at <https://github.com/bassoy/ttm>. The sequential tensor-matrix multiplication of TLIB is part of uBLAS and in the official release of `Boost v1.70.0` and later.

References

- [1] E. Karahan, P. A. Rojas-López, M. L. Bringas-Vega, P. A. Valdés-Hernández, P. A. Valdes-Sosa, Tensor analysis and fusion of multimodal brain images, *Proceedings of the IEEE* 103 (9) (2015) 1531–1559.
- [2] E. E. Papalexakis, C. Faloutsos, N. D. Sidiropoulos, Tensors for data mining and data fusion: Models, applications, and scalable algorithms, *ACM Transactions on Intelligent Systems and Technology (TIST)* 8 (2) (2017) 16.
- [3] N. Lee, A. Cichocki, Fundamental tensor operations for large-scale data analysis using tensor network formats, *Multidimensional Systems and Signal Processing* 29 (3) (2018) 921–960.
- [4] T. G. Kolda, B. W. Bader, Tensor decompositions and applications, *SIAM review* 51 (3) (2009) 455–500.
- [5] B. W. Bader, T. G. Kolda, Algorithm 862: Matlab tensor classes for fast algorithm prototyping, *ACM Trans. Math. Softw.* 32 (2006) 635–653.
- [6] E. Solomonik, D. Matthews, J. Hammond, J. Demmel, Cyclops tensor framework: Reducing communication and eliminating load imbalance in massively parallel contractions, in: *Parallel & Distributed Processing (IPDPS)*, 2013 IEEE 27th International Symposium on, IEEE, 2013, pp. 813–824.
- [7] P. Springer, P. Bientinesi, Design of a high-performance gemm-like tensor-tensor multiplication, *ACM Transactions on Mathematical Software (TOMS)* 44 (3) (2018) 28.
- [8] D. A. Matthews, High-performance tensor contraction without transposition, *SIAM Journal on Scientific Computing* 40 (1) (2018) C1–C24.
- [9] E. D. Napoli, D. Fabregat-Traver, G. Quintana-Ortí, P. Bientinesi, Towards an efficient use of the blas library for multilinear tensor contractions, *Applied Mathematics and Computation* 235 (2014) 454 – 468.
- [10] J. Li, C. Battaglini, I. Perros, J. Sun, R. Vuduc, An input-adaptive and in-place approach to dense tensor-times-matrix multiply, in: *High Performance Computing, Networking, Storage and Analysis*, 2015, IEEE, 2015, pp. 1–12.
- [11] Y. Shi, U. N. Niranjan, A. Anandkumar, C. Cecka, Tensor contractions with extended blas kernels on cpu and gpu, in: *2016 IEEE 23rd International Conference on High Performance Computing (HiPC)*, 2016, pp. 193–202.
- [12] C. Bassoy, Design of a high-performance tensor-vector multiplication with blas, in: *International Conference on Computational Science*, Springer, 2019, pp. 32–45.
- [13] F. Pawłowski, B. Uçar, A.-J. Yzelman, A multi-dimensional morton-ordered block storage for mode-oblivious tensor computations, *Journal of Computational Science* 33 (2019) 34–44.
- [14] A. Paszke, S. Gross, F. Massa, A. Lerer, J. Bradbury, G. Chanan, T. Killeen, Z. Lin, N. Gimelshein, L. Antiga, et al., Pytorch: An imperative style, high-performance deep learning library, *Advances in neural information processing systems* 32 (2019).
- [15] L.-H. Lim, Tensors and hypermatrices, in: L. Hogben (Ed.), *Handbook of Linear Algebra*, 2nd Edition, Chapman and Hall,

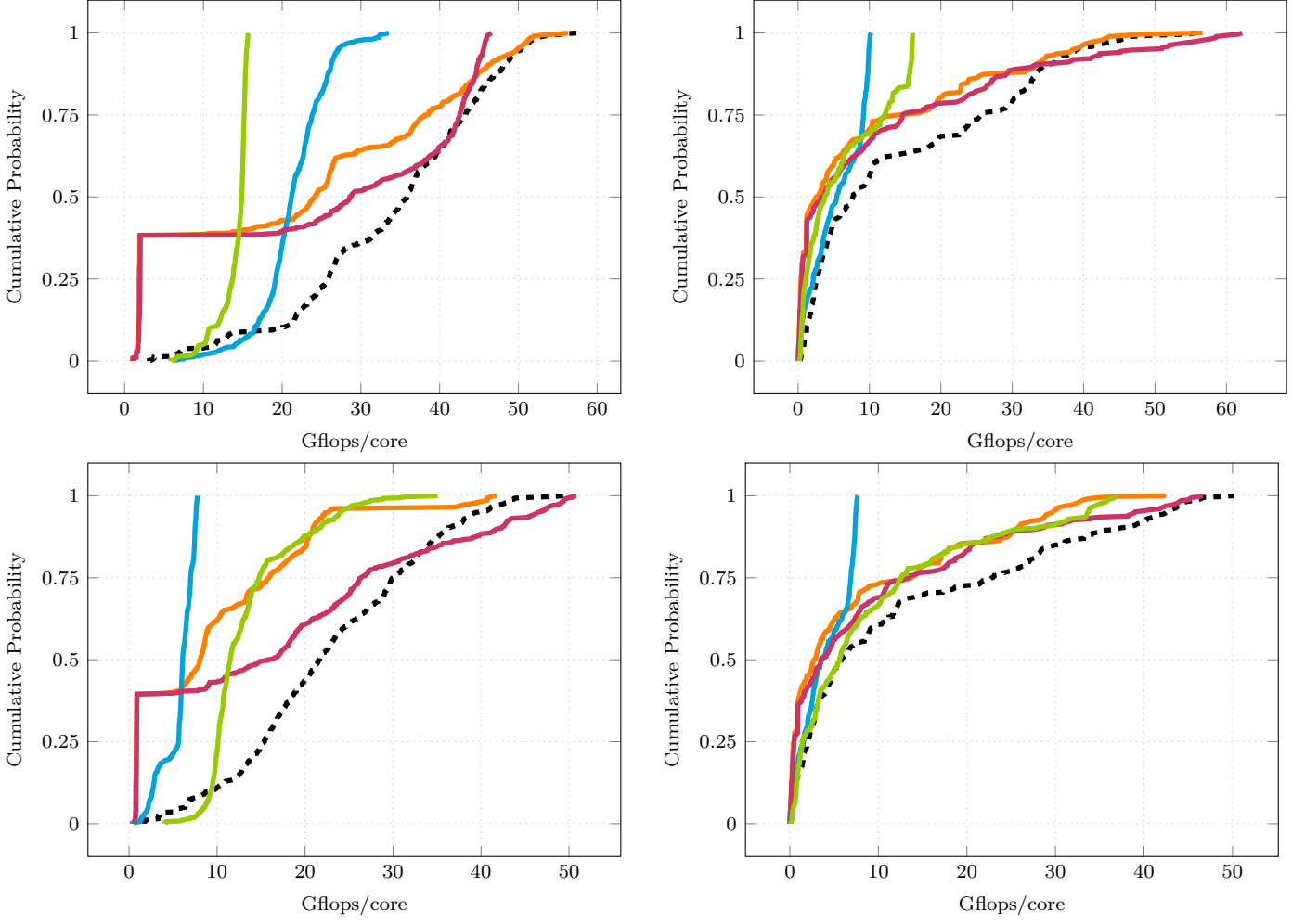


Figure 4: Cumulative performance distributions of tensor-times-matrix algorithms in double-precision Tflops. Each distribution line belongs to a library: **tlib**[ours] (---), **tcl** (—), **tblis** (—), **libtorch** (—), **eigen** (—). Libraries have been tested with asymmetrically-shaped (left plot) and symmetrically-shaped tensors (right plot).

- 2017.
- [16] C. Basso, V. Schatz, Fast higher-order functions for tensor calculus with tensors and subtensors, in: International Conference on Computational Science, Springer, 2018, pp. 639–652.
 - [17] J. Cohen, C. Basso, L. Mitchell, Ttv in tensorly, Tensor Computations: Applications and Optimization (2022) 11.
 - [18] J. Kossaifi, Y. Panagakis, A. Anandkumar, M. Pantic, Tensorly: Tensor learning in python, Journal of Machine Learning Research 20 (26) (2019) 1–6.